Published in Photonics Technology Letters (IEEE) 14, issue 1, 18-20, 2002
which should be used for any reference to this work

Distributed-Feedback Quantum Cascade Lasers Emitting in the 9-μm Band With InP Top Cladding Layers

Daniel Hofstetter, Mattias Beck, Thierry Aellen, Jérôme Faist, *Member, IEEE*, Ursula Oesterle, Marc Ilegems, *Member, IEEE*, Emilio Gini, and Hans Melchior, Life Fellow, IEEE

***Abstract*—Two different high performance quantum cascade distributed-feedback lasers with four quantum-well-based active regions and InP top cladding layers are presented. The first device, which emitted at 9.5 μm, was mounted junction down in order to get high average powers of up to 71 mW at −30 °C and 30 mW at room temperature. The other device, which lased at 9.1μm, was optimized for high pulsed operating temperatures and tested up to 150 °C at 1.5% duty cycle. The emission of both lasers stayed single mode with more than 20-dB side-mode suppression ratio over the entire investigated power and temperature range.**

***Index Terms*—Distributed feedback, high power, high temperature, mid-infrared, quantum cascade laser.**

IN RECENT YEARS, different spectroscopic techniques in the mid-infrared (mid-IR) wavelength range have suffered from the absence of convenient semiconductor light sources. Lead salt lasers exist already for a long time, but their highest operating temperature could not be pushed beyond 220 K [1]. In addition, even at cryogenic temperatures, their output power remained relatively small, in the range of a couple of milliwatts [2]. Although room-temperature quantum cascade (QC) distributed feedback (DFB) lasers are so far available only in pulsed operation, their much higher average output power has made them very interesting light sources for spectroscopic applications [3], [4]. A variety of different experimental configurations and emission wavelengths has been published in the last couple of years, among them photoacoustic spectroscopy [5], and single-pass or multiple-pass absorption spectroscopy [6]. Recently, we succeeded in fabricating a high-power 5.3-μm DFB QC laser with surface grating technology. Thanks to an active region design based on a two phonon resonance, this device exhibited peak powers in the 1-W range and could be operated at high temperatures of up to 120 °C [7]. Here, we report on two similar DFB lasers emitting in the 9-μm band; they use the same two phonon resonance architecture as the 5.3-μm device described above, but are equipped with a regrown InP top cladding layer over the grating. Since InP has a much higher thermal conductivity and a lower refractive index than the formerly used InAlAs top cladding layer, the thermal resistance and the modal overlap of the laser will be greatly improved. With respect to devices using ternary cladding layers, the performance is, thus, superior in terms of high duty cycle and/or high temperature operation. The first laser was optimized for high duty cycle and high average power operation (up to 71 mW at 16% duty cycle and −30 °C), while the second laser showed excellent tuning and high-temperature characteristics up to 150 °C.

The fabrication of these lasers relied on molecular beam epitaxy (MBE) for the active region and the waveguide layers, and metal-organic vapor phase epitaxy (MOVPE) for the top cladding and contact layers. Molecular beam epitaxy growth started with the lower waveguide layer ($In_{0.53}Ga_{0.47}As$, Si, 6×10^{16} cm^{-3}, total thickness 0.225 μm) on an n-doped InP (Si, 2×10^{17} cm^{-3}) substrate, proceeded with an active region (thickness 1.82 μm) and was finished by an upper waveguide layer ($In_{0.53}Ga_{0.47}As$, Si, 6×10^{16} cm^{-3}, thickness 0.23 μm). Sample S1810 received then a grating with a period of 1.528 μm, while the grating period of sample S1850 was 1.428 μm. Both gratings were chemically wet-etched to a depth of 190 nm using an H_3PO_4–H_2O_2–H_2O (2 : 4 : 6) solution. After thorough cleaning of the surface, the samples were transferred to an MOVPE system, where the top cladding layer (InP, Si, 1×10^{17} cm^{-3}, thickness 2.5 μm), the contact layer (InP, Si, 7×10^{18} cm^{-3}, thickness 0.85 μm), and the cap layer (InP, Si, 1×10^{20} cm^{-3}, thickness 10 nm) were grown. The active region, which formed the central part of the waveguide, consisted of 35 periods; those were alternating n-doped funnel injector regions and undoped four quantum-well (QW) gain regions. Typical electron scattering times and dipole matrix elements as well as a general description of a four QW (or two phonon resonance) design have been discussed in detail in [7]. The layer sequence of sample S1810 in nanometers, and starting from the injection barrier, was **3.8**/2.1/**0.7**/6.3/**0.9**/5.9/**0.9**/5.4/**2.2**/3.6/**1.4**/3.4/**1.4**/3.2/**1.8**/3.1/**2.0**/3.1 nm. $In_{0.52}Al_{0.48}As$ barrier layers are in bold, $In_{0.53}Ga_{0.47}As$ well layers are in roman, and n-doped layers (Si 3×10^{17} cm^{-3} for S 1810) are underlined. Sample S1850 had its lasing transition at a slightly higher energy and used, therefore, an injector with seven well/barrier pairs. Its layer structure has been published in [8]. Laser fabrication using ridge waveguide etching, Si_3N_4 deposition, metallization, and thinning proceeded then by standard procedures. In order to have a large thermal conductance, device S1810 was mounted junction down on a copper

D. Hofstetter, M. Beck, T. Aellen, and J. Faist are with the University of Neuchâtel, Institute of Physics, Neuchâtel, CH 2000, Switzerland.

U. Oesterle and M. Ilegems are with IMO, Physics Department, EPFL, Ecublens, 1015 Lausanne, Switzerland.

E. Gini and H. Melchior are with the Institute of Quantum Electronics, ETHZ, 8093 Zürich, Switzerland.

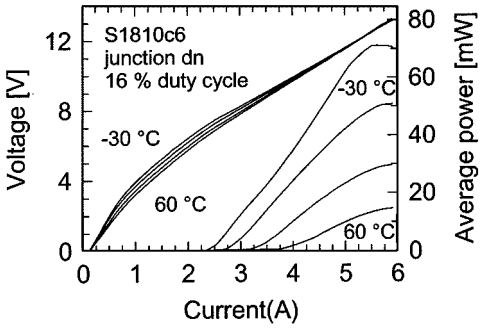

Fig. 1. Series of L–I and I–V curves of a 26-μm-wide and 1.5-mm-long DFB laser taken from the sample S1810 and at different temperatures between -30 °C and 60 °C. For this particular measurement, a duty cycle of 16% (45-ns pulse length/3.6-MHz pulse repetition frequency) was used.

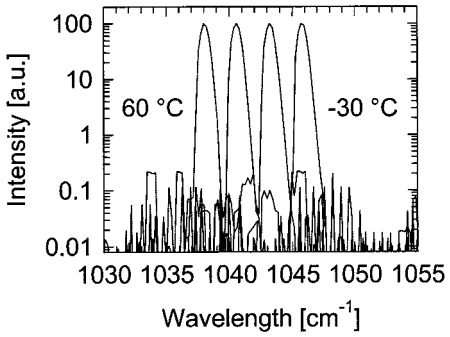

Fig. 2. Series of emission spectra of a 26-μm wide and 1.5-mm long DFB laser taken from the sample S1810 and at different temperatures between -30 °C and 60 °C. Each spectrum was measured at the maximum output power at 16% duty cycle.

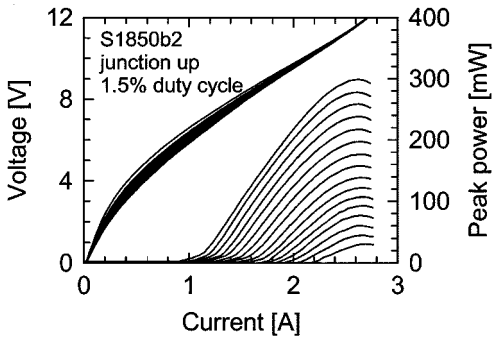

Fig. 3. Series of L–I and I–V curves of a 24-μm-wide and 1.5-mm-long DFB laser taken from the sample S1850 and at different temperatures between -20 °C and 13 °C (spacing 10 °C). For this particular measurement, a duty cycle of 1.5% (45-ns pulselength/333-kHz pulse repetition frequency) was used.

heatsink. This allowed, especially at high duty cycle, a very efficient extraction of the produced heat. Since we tested the other device (S1850) only at high temperature, but not at high duty cycle, junction up mounting worked sufficiently well. In both cases, a 2-μm thick thermally evaporated In layer was used for soldering.

For testing, the devices were placed into a Peltier-cooled aluminum box with an antireflection coated ZnSe-window (Alpes Lasers SA). Average output power and voltage versus current (L–I–V) curves at temperatures between -30 and 150 °C could be measured in this configuration. A pulse length of 45 ns was used with a variable pulse repetition frequency in order to achieve a duty cycle between 0.1% ($f_{\mathrm{rep}} = 22$ kHz) and 16% ($f_{\mathrm{rep}} = 3.6$ MHz). For the acquisition of emission spectra at high duty cycle (sample S1810), we collected the light with an Au-coated parabolic off-axis mirror (60°, $f/1.33$). After reflection on a second parabolic mirror (90°, $f/3.75$), the light was focused onto the input slit of a grating spectrometer (Jobin–Yvon, $d_{\mathrm{focal}} = 0.3$ m). At low duty cycle (S1850), a Fourier transform spectrometer was used instead of the grating spectrometer.

Fig. 1 shows a series of L–I- and I–V curves of a 26-μm wide and 1.5-mm long DFB laser taken from sample S1810. For this particular measurement, a duty cycle of 16% was used. The emitted average power was 71 mW at -30 °C and 15 mW at 60 °C. At 1.5% duty cycle, we observed maximal slope efficiencies of 194 mW/A at -30 °C and 93 mW/A at 60 °C. The corresponding threshold currents were 2.3 A and 3.34 A; these values are equivalent to threshold current densities of 5.9 kA/cm^2 and 8.55 kA/cm^2 at the respective temperatures. The characteristic temperature T_0, which empirically describes the behavior of the threshold current as a function of the temperature was 243 K. Exact matching between Bragg and gain peak was achieved at 40 °C; this led to a T_0 value which was somewhat better than the one observed with the Fabry–Pérot laser fabricated from the same material ($T_{0\mathrm{Fabry-Pérot}} = 183$ K). At 16% duty cycle, the threshold currents were 2.7 A for -30 °C and 4.4 A for 60 °C; giving rise to a slightly lower T_0 value of 184 K. From the threshold current values at low and high duty cycle and the T_0 at low duty, one can estimate the temperature increase ΔT in the active region with respect to the copper heatsink. This calculation shows that for higher temperatures, the laser active region heats faster than the heatsink ($\Delta T = 39$ K at -30 °C and $\Delta T = 67$ K at 60 °C). This is also illustrated by the slightly elevated temperature tuning coefficient, which can be derived from the spectra shown in Fig. 2. These spectra are measured at 16% duty cycle and the maximal output power for each temperature. The laser can be continuously tuned from 1046 cm^{-1} at -30 °C to 1038 cm^{-1} at 60 °C with a tuning coefficient of $1/\beta \times \Delta\beta/\Delta T = -8.5 \times 10^{-5}$ K^{-1}. Due to the overheating of the active region, this value is about 22% larger than expected from the temperature-induced refractive index change [9]. The spectral width of about 1 cm^{-1} is due to the duration of the electrical pulses; for shorter electrical pulses, we observed a proportional linewidth narrowing [5]. The sidemode suppression ratio was on the order of 20 dB for the entire investigated temperature range.

For the second DFB laser, which was fabricated from sample S1850, L–I- and I–V curves as a function of temperature are presented in Fig. 3. This device was 24 μm wide and 1.5 mm long. The curves are obtained at 1.5% duty cycle in order to demonstrate the excellent high temperature capability of the material. The highest temperature for which we could reliably measure the L–I–V curve was 130 °C. The threshold current increase from 0.95 A at -20 °C to 2.2 A at 130 °C corresponds to a characteristic temperature of 179 K. In contrast to the device presented above, this laser had the exact match between Bragg resonance and gain peak at -20 °C. This resulted in a slightly worse T_0 value compared to the Fabry–Pérot laser fabricated from the same material ($T_{0\mathrm{Fabry-Pérot}} = 226$ K). At

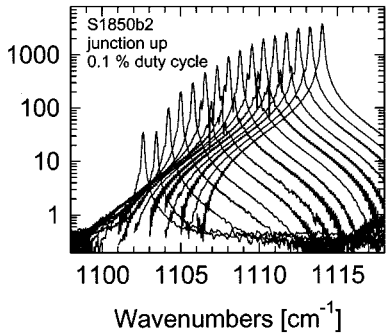

Fig. 4. Series of emission spectra of a 24-μm-wide and 1.5-mm-long DFB laser taken from the sample S1850 and at different temperatures between 0 °C and 150 °C (spacing 10 °C). Each spectrum was measured at an injection current of 2.5 A and at 0.1% duty cycle.

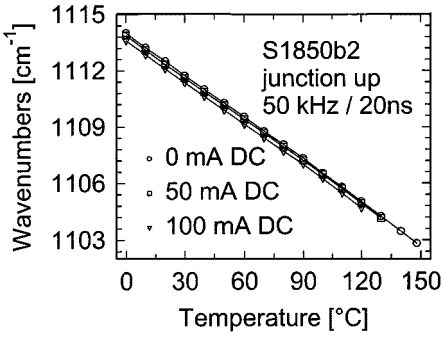

Fig. 5. Emission wavelength as a function of temperature of a DFB laser S1850. The three curves correspond to the three different cases with a dc bias of 0, 50, and 100 mA.

-20 °C, we observed a slope efficiency of 187 mW/A with a rollover power of 300 mW; while at 130 °C, 62 mW/A and 47 mW were seen. In Fig. 4, we present the emission spectra measured at temperatures between 0 °C and 150 °C and a current of 2.5 A. The duty cycle for this series of measurements was 0.1% with 20-ns long pulses and a repetition rate of 50 kHz. Depending on the heatsink temperature, a sidemode suppression ratio of at least 20 dB was seen. The emission peak shifted continuously from 1114 cm^{-1} at 0 °C to 1102.4 cm^{-1} at 150 °C. This is equivalent to a temperature tuning coefficient of $1/\beta \times \Delta\beta/\Delta T = -6.95 \times 10^{-5}$ K^{-1}. At low temperatures, where the operating current of 2.5 A was much larger than the threshold current, the laser suffered somewhat from chirping. This led to a small shoulder on the long wavelength side (i.e., the small wavenumber side) of the main peak.

The high operating temperature of these DFB lasers could be used to investigate the temperature dependence of the thermal conductivity of the S1850 laser material. For this purpose, we measured another two series of emission spectra under slightly different conditions. The results of these experiments are shown in Fig. 5. In the first experiment, the baseline of the electrical pulses was shifted from 0 to 50 mA. This is equivalent to having a 50-mA dc bias, on top of which we added a pulsed signal 50 mA smaller than before. For each temperature and a total current of 2.5 A, the wavelength was compared to the one obtained at normal conditions (no dc bias). In the second measurement, we increased the dc bias to 100 mA and measured again the emission wavelength for each temperature. The dc bias-induced heating caused a measurable wavelength shift of the DFB laser. For each given temperature, this wavelength shift (or temperature increase) remained at a constant value of -0.12 cm^{-1} for 50 mA dc bias ($V_{\rm device} = 2.5$ V) and -0.36 cm^{-1} for 100 mA dc bias ($V_{\rm device} = 3.5$ V). Since a constant temperature increase was observed for all investigated temperatures (when adding a certain dc bias), we can conclude that the thermal conductivity remained unchanged with increasing temperature. From the additional power to be dissipated and the observed temperature increase, we can calculate the thermal resistance using $R_{th} = \Delta T/(V_{\rm device} \times I_{\rm dc})$; this yields $R_{\rm th} = 14.7$ K/W or (taking into account the area of the laser) $g_{\rm th} = 190$ W·K cm^2.

In conclusion, we have demonstrated two different single-mode QC DFB lasers based on a design with a double phonon resonance in the active region. While the first device was mounted junction down, and thus, optimized for high average power and high duty cycle operation, the second laser was soldered junction up and could be driven at elevated temperatures of up to 150 °C.

Acknowledgment

The authors gratefully acknowledge the technical assistance of S. Blaser and M. Rochat.

References

[1] M. Tacke, "New developments and applications of tunable IR lead salt lasers," *Infrared Phys. Technol.*, vol. 36, pp. 447–463, 1995.

[2] G. Springholz, T. Schwarzl, M. Aigle, H. Pascher, and W. Heiss, "4.8 μm vertical emitting PbTe quantum-well lasers based on high-finesse EuTe/$Pb_{1-x}Eu_xTe$ microcavities," *Appl. Phys. Lett.*, vol. 76, pp. 1807–1809, 2000.

[3] C. Gmachl, F. Capasso, J. Faist, A. L. Hutchinson, A. Tredicucci, D. L. Sivco, J. N. Baillargeon, S. N. G. Chu, and A. Y. Cho, "Continuous wave and high power pulsed operation of index-coupled distributed feedback quantum cascade lasers," *Appl. Phys. Lett.*, vol. 72, pp. 1430–1432, 1998.

[4] R. Köhler, C. Gmachl, A. Tredicucci, F. Capasso, D. L. Sivco, S.-N. G. Chu, and A. Y. Cho, "Single-mode tunable, pulsed, and continuous wave quantum-cascade distributed feedback lasers at $\lambda = 4.6$–$4.7\,\mu$m," *Appl. Phys. Lett.*, vol. 76, pp. 1092–1094, 2000.

[5] D. Hofstetter, M. Beck, J. Faist, M. Nägele, and M. W. Sigrist, "Photo-acoustic spectroscopy with quantum cascade distributed feedback lasers," *Optics Lett.*, vol. 26, pp. 887–889, 2001.

[6] P. Hess, "Principles of photoacoustic and photothermal detection in gases," in *Principles and Perspectives of Photothermal and Photoacoustic Phenomena*, A. Mandelis, Ed. New York: Elsevier, 1992, ch. 4.

[7] D. Hofstetter, M. Beck, T. Aellen, and J. Faist, "High-temperature operation of distributed feedback quantum-cascade lasers at 5.3 μm," *Appl. Phys. Lett.*, vol. 78, pp. 396–398, 2001.

[8] D. Hofstetter, M. Beck, T. Aellen, J. Faist, U. Oesterle, M. Ilegems, E. Gini, and H. Melchior, "Continuous wave operation of a 9.3 μm quantum cascade laser on a Peltier cooler," *Appl. Phys. Lett.*, vol. 78, pp. 1964–1966, 2001.

[9] J. Faist, C. Gmachl, F. Capasso, C. Sirtori, D. L. Sivco, J. N. Baillargeon, and A. Y. Cho, "Distributed feedback quantum cascade lasers," *Appl Phys. Lett.*, vol. 70, pp. 2670–2672, 1997.